Imaging of C-X-C Motif Chemokine Receptor CXCR4 Expression After Myocardial Infarction With [^{68}Ga] Pentixafor-PET/CT in Correlation With Cardiac MRI

C-X-C motif chemokine receptor 4 (CXCR4) and its ligand stromal cell-derived factor-1α have been shown to be involved in the orchestration of post-infarct inflammation and its resolution in patients with acute myocardial infarction (AMI) (1). Recently, pilot visualization of CXCR4-expression using a radiolabeled PET ligand ([^{68}Ga]Pentixafor) could be demonstrated in patients after AMI (2,3). The aim of this study was to further investigate CXCR4 expression after myocardial ischemia in comparison to cardiac magnetic resonance (CMR).

From January 2015 to June 2016, 22 patients (17 men and 5 women, mean age 61 ± 11 years) with (sub) acute myocardial infarction underwent imaging with [^{68}Ga]Pentixafor-positron emission tomography (PET)/computed tomography (CT) and CMR (21 patients, 1 patient excluded because of *adipositas permagna*) within 2 to 13 days after onset of symptoms (median delay between PET and CMR: 1 day). Thirteen patients returned for follow-up CMR (1 to 14 months; median: 4 months). A total of 75 ± 15 min after injection of 116 ± 29 MBq of [^{68}Ga]Pentixafor, PET/CT was performed (2). Images were first inspected visually. For semi-quantitative analysis, the axial PET image slice with maximum cardiac uptake was selected. A standardized 10-mm circular region was placed over the area with the peak activity to derive maximum and peak standardized uptake values. For signal-to-background ratios, peak standardized uptake values were also derived in normal reference regions by a second region of interest (diameter: 10 mm) in a remote region of the left ventricular wall without late-gadolinium-enhancement (LGE) in the corresponding CMR data. For multi-organ analysis of [^{68}Ga]Pentixafor uptake, mean standardized uptake values were also derived for bone marrow (thoracic vertebrae) and spleen. These PET parameters were then correlated with clinical (creatine kinase [CK], troponin T, leukocyte, and C-reactive protein levels) as well as with CMR parameters.

CMR was performed on a 1.5-T (n = 7) (Achieva 1.5-T, Philips Healthcare, Best, the Netherlands) and 3.0-T (n = 15) (Achieva DS 3.0-T, Philips Healthcare) scanner using dedicated protocols (2). In analogy to PET, LGE and T2-weighted images were analyzed for necrosis/Scar and edema, respectively (17-segment model). Concordant signal enhancement in both LGE and T2-weighted sequences was considered as CMR-positive for acute cardiac damage. LGE positivity associated with T2 negativity was rated as consistent with fibrotic changes.

Statistical analyses were performed using PASW Statistics software version 22.0 (SPSS, Inc., Chicago, Illinois). Quantitative values were expressed as mean ± SD or median and range as appropriate. Comparisons of related metric measurements were performed using the Wilcoxon-signed rank test. The chi-square or Fisher exact test was conducted for comparison of frequency data between independent subgroups. For bivariate correlation analyses, Pearson correlation coefficients were calculated. All statistical tests were performed 2-sided and a p value <0.05 was considered to indicate statistical significance. No correction was applied for p values to adjust for multiple tests.

On visual inspection, [^{68}Ga]Pentixafor-PET was positive in 17 of 22 patients with AMI. On a segment basis, 65 of 306 segments were rated positive, concordant to CMR. Infarct-to-remote ratios were 2.2 ± 0.4 and infarct-to-left cavity ratios were 1.4 ± 0.1. CXCR4 expression could be observed up to 13 days after AMI and was negatively correlated with time after onset of symptoms ($r = -0.73$; $p < 0.01$). CXCR4 expression was not related to myocardial damage as assessed by initial troponin T or CK levels (all $p > 0.40$; all $r > -0.24$ and <0).

Regarding the systemic inflammatory response, CXCR4 expression in the bone marrow correlated with serum leukocyte levels ($r = 0.64$; $p < 0.01$). Splenic tracer uptake showed a negative correlation with organ size ($r = -0.51$; $p = 0.03$), CK levels ($r = -0.62$; $p < 0.01$) and with necrotic tissue volume ($r = -0.67$; $p < 0.01$). [^{68}Ga]Pentixafor uptake and serum C-reactive protein levels showed no significant correlation (p = NS).

CXCR4 expression in the infarct area showed a negative correlation to scar volume at follow-up (normalized to body surface area, $r = -0.64$; $p = 0.03$) (**Figure 1**). [^{68}Ga]Pentixafor uptake in the bone marrow correlated with better healing of the initial ischemic volume ($r = -0.70$; $p < 0.01$). Spleen standardized uptake values were negatively related with necrosis volume ($r = -0.70$; $p < 0.01$) and showed a positive correlation with ejection fraction at follow-up ($r = 0.75$; $p < 0.01$) and the change of ejection fraction ($r = 0.72$; $p < 0.01$) (**Figure 1**) when compared with baseline.

The current report of in vivo imaging of CXCR4 in the human heart demonstrates the feasibility of

FIGURE 1 Correlations Between CXCR4 Expression Imaged by Positron Emission Tomography and Cardiac Magnetic Resonance-Derived Myocardial Outcome Parameters

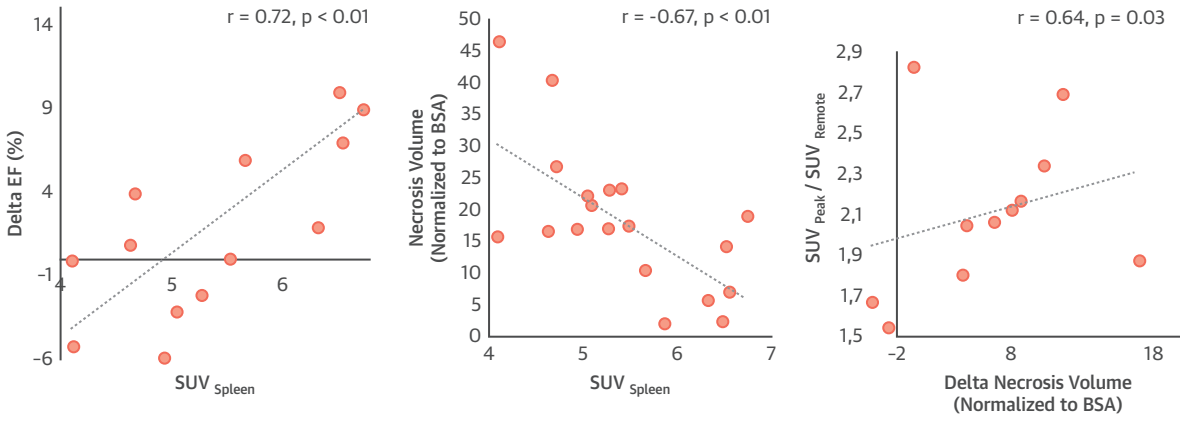

Necrosis volume (normalized to BSA) is given in cm^3/m^2. AMI = acute myocardial infarction; BSA = body surface area; Delta EF = ejection fraction at follow-up minus ejection fraction at time point of acute myocardial infarction; EF = ejection fraction; SUV = standardized uptake value.

noninvasive chemokine receptor imaging up to 2 weeks after AMI. [^{68}Ga]Pentixafor uptake in the infarcted myocardium strongly correlated with the time point of imaging with a linear decline up to day 13 after myocardial ischemia. Our findings, in parallel to the literature (3), suggest that infiltrating inflammatory cells can be assumed the major cellular source of the PET signal, potentially triggering a beneficial immune response (also evidenced by CXCR4 activation in bone marrow and spleen) that results in myocardial healing. Correspondingly, CXCR4 expression in the infarcted area also correlated with smaller scar volumes at follow-up.

This study has various limitations. First, a relatively small number of patients could be analyzed. Time points of PET and CMR imaging varied. No longitudinal CXCR4 imaging of the individual patients could be obtained. Molecular inflammatory endpoints including CXCR4/CXCL12 levels in the periphery were not assessed, and comparisons to imaging endpoints could not be performed. Histological proof of the cellular origin of the PET signal cannot be provided. Because CXCR4 expression was detected up to 2 weeks after the acute event, it cannot be excluded that at least a small fraction of the signal may stem from resident cells including cardiomyocytes, fibroblasts, endothelial cells or progenitor cells that were recruited to the damaged tissue (4,5).

In conclusion, this study suggests that CXCR4 expression after AMI as assessed by [^{68}Ga]Pentixafor-PET is capable of revealing the myocardial healing potential. The investigation of underlying (patho) physiological mechanisms is a subject for further studies.

Theresa Reiter, MD
Malte Kircher, MD
Andreas Schirbel, PhD
Rudolf A. Werner, MD
Saskia Kropf, MEng
Georg Ertl, MD
Andreas K. Buck, MD
Hans-Jürgen Wester, PhD
Wolfgang R. Bauer, PhD, MD
Constantin Lapa, MD*

*Department of Nuclear Medicine
University Hospital Würzburg
Oberdürrbacher Strasse 6
97080 Würzburg
Germany
E-mail: lapa_c@ukw.de

https://doi.org/10.1016/j.jcmg.2018.01.001

Please note: Dr. Wester is founder and shareholder, of Scintomics. Ms. Kropf is CEO of Scintomics. All other authors have reported that they have no relationships relevant to the contents of this paper to disclose. Drs. Reiter and Kircher contributed equally to this work and are joint first authors. Drs. Bauer and Lapa contributed equally to this work and are joint senior authors.

REFERENCES

1. Doring Y, Pawig L, Weber C, Noels H. The CXCL12/CXCR4 chemokine ligand/receptor axis in cardiovascular disease. Front Physiol 2014;5:212.

2. Lapa C, Reiter T, Werner RA, et al. [(68)Ga]Pentixafor-PET/CT for imaging of chemokine receptor 4 expression after myocardial infarction. J Am Coll Cardiol Img 2015;8:1466–8.

3. Thackeray JT, Derlin T, Haghikia A, et al. Molecular imaging of the chemokine receptor CXCR4 after acute myocardial infarction. J Am Coll Cardiol Img 2015;8:1417–26.

4. Hu X, Dai S, Wu WJ, et al. Stromal cell derived factor-1 alpha confers protection against myocardial ischemia/reperfusion injury: role of the cardiac stromal cell derived factor-1 alpha CXCR4 axis. Circulation 2007; 116:654–63.

5. Saxena A, Fish JE, White MD, et al. Stromal cell-derived factor-1alpha is cardioprotective after myocardial infarction. Circulation 2008;117:2224–31.

Fusion Imaging During the Interventional Closure of Patent Foramen Ovale and Atrial Septal Defects

Mandatory or Superfluous?

Real-time fusion imaging has emerged as a sophisticated tool to guide structural heart disease (SHD) interventions. The overlay of 2 different imaging modalities allows the interventionalist to visualize echocardiographic images within a fluoroscopic image that offers intuitive perception of the anatomy, the catheters, and devices in real-time (**Figure 1**). This approach may facilitate SHD interventions, where continuous tissue anatomy information is essential.

We retrospectively analyzed 141 consecutive patients who underwent closure of either patent foramen ovale (PFO) or an atrial septal defect (ASD) before (EN- group; n = 36) or after (EN+ group; n = 105) the introduction of the fusion imaging software (EchoNavigator Release II [EN], Philips Healthcare, Amsterdam, the Netherlands). The EN software is based on the real-time coregistration and visualization of transesophageal echocardiography (TEE) and fluoroscopy data and has been described previously (1). Procedure-related endpoints included technical success, procedure time, fluoroscopy time, and dose-area product. Technical success was defined as delivery and release of the device (2). Safety-related endpoints included the occurrence of in-hospital adverse events, which were classified according to the RESPECT (Randomized Evaluation of Recurrent Stroke Comparing PFO Closure to Established Current Standard of Care Treatment) trial (2). Echocardiographic follow-up data were obtained at 3 and 6 months.

Procedural success was achieved in 97.2% of the patients in the EN+ group and in 100% of the patients in the EN- group (p = 1.0). In 1 patient of the EN+ group, the device could not be positioned as the ASD was too large and presented an insufficient posterior rim. The median procedure time was 41 min (interquartile range [IQR]: 28.25 to 50.0) in the EN- group and 40 min (IQR: 31 to 56) in the EN+ group (p = 0.964). There were no differences between the EN- and EN+ groups with regard to fluoroscopy time (6.0 min [IQR: 3.9 to 8.98] vs. 5 min [IQR: 4 to 9]; p = 0.530) and dose-area product (1,078 cGy · cm^2 [IQR: 657.875 to 2,091.175] vs. 1,521.4 cGy · cm^2 [IQR: 988.1 to 2,700.5]; p = 0.193). One patient (2.8%) in the EN- group developed intraprocedural atrial fibrillation; no intraprocedural events were observed in the EN+ group. During the post-interventional course, minor bleeding occurred in 3 patients (2.9%) in the EN+ group; no adverse in-hospital events were observed in the EN- group. Follow-up at 3 and 6 months, including a TEE, was performed in all patients (100%). In 1 patient (0.9%) in the EN+ group, a residual shunt was found (p = 1.0). No adverse events were documented in both groups.

For the first time, fusion imaging was compared with standard TEE in an adult PFO/ASD cohort. We found that the application of fusion imaging is safe and feasible during the closure of PFO/ASD, but no differences in procedure time, fluoroscopy time, or dose-area product were observed between groups.

It could be assumed that fusion imaging is not able to show a measurable advantage in PFO/ASD closure due to the highly standardized and rather simple interventional approach. Anatomical orientation during these procedures is less complex and can be accurately provided by standard TEE, differently from more complex SHD procedures.

Recently, we demonstrated that the time until transseptal puncture was decreased using fusion imaging during left atrial appendage closure and the MitraClip (Abbott, Chicago, Illinois) procedure (3). In a previous study, radiation time was significantly reduced in patients undergoing left atrial appendage closure using fusion imaging (4). In these challenging interventions, the additional information given by fusion imaging may facilitate the procedure and improve the confidence of the interventionalist. From this perspective, the application of fusion imaging during the interventional closure of PFO/ASD might not be mandatory, but it has an educational and training effect that might be advantageous for more complex SHD interventions.

Our study has some limitations. First, it was a retrospective design and therefore the results have to be evaluated in prospective trials. Second, the unequal size of both groups does not allow a matched-pair analysis. Before the introduction of EN release II we worked with EN release I, which depicts only markers and offers no real-time fusion imaging. However, these patients had to be excluded from our analysis, resulting in a smaller patient cohort without the use of fusion imaging.